

Analysis of the Elastic Stress-Strain Behavior of Complex-Shaped Three-Dimensional Bodies

Muhammadaziz Rasulmammedov^{1,2}, Shokhsanam Shukurova^{1,2} and Zamira Mirzayeva^{1,2}

¹ Department of Information Systems and Technologies in Transport, Tashkent State Transport University,
Temiryolchilar Str. 1, 100167 Tashkent, Uzbekistan

² University of Diyala, 32009 Baqubah, Diyala, Iraq
prof.rasulmukhamedov@gmail.com, shoxsanamm2896@gmail.com, zmirzaeva83@mail.ru

Keywords: Three-Dimensional Bodies, Elastoplastic Process, Finite Elements, Finite Difference, Vlasov-Kantorovich Method.

Abstract: The problem of the bending of a parallelepiped under external forces was examined using the finite element method. The given three-dimensional Lamé equations were transformed into a symmetric algebraic system by applying the finite element method, and then solved using the square root method. As a result, the three displacements u_1 , u_2 , u_3 and the six stress components σ_{11} , σ_{22} , σ_{33} , σ_{12} , σ_{13} , σ_{23} were determined for various external forces and the height of the body. The formulation of three-dimensional elastoplastic problems, the application of finite element methods, Vlasov-Kantorovich, and finite difference methods in the calculation of bodies with complex three-dimensional shapes (with cavities, appendages, and depressions) is presented along with algorithms for solving the systems of equations and calculating the coefficients. By using a combination of theoretical analysis and numerical simulations, we study the interrelationship between elastic and plastic behaviors under various loading conditions. The research emphasizes the significance of the material properties, geometric configuration, and boundary conditions in influencing the modes of deformation.

1 INTRODUCTION

In the last decade, the Vlasov-Kantorovich method, the finite difference method (FDM), and the finite element method (FEM) have become some of the most widely used techniques for solving problems in the mechanics of deformable solids on computers. This is explained by the fact that practically any problem, regardless of complexity, can be modeled using these methods; however, this results in a system of equations with a very high order. Solving such large-order systems has become feasible in the last decade, associated with the development of computer technologies. On the other hand, this method allows transforming large (two-dimensional, three-dimensional) problems into a series of smaller problems that can be solved sequentially, thereby reducing the order of the initial system of equations [1]. This significantly simplifies the creation of efficient algorithms for solving these problems. Although the existence of this effect is acknowledged, relatively little research has been done on how the relative positions of finite elements affect the quality of the numerical solutions that are

obtained. Numerical methods' approximation and convergence can be enhanced by effectively controlling computational components. The basics of building and utilizing three-dimensional open work schemes based on the approximation of variational equations (including finite element technique schemes) are illustrated in works [1] and [2]. A portion of a traditional isoparametric parallelepiped can be removed to create open networks of finite elements, which form the basis of such systems. In this situation, it is possible to minimize the number of computational cells by at least three times.

2 FORMULATION OF THE PROBLEM

To calculate any structure, it is necessary to start by forming its calculation scheme. This means that the representation of the construction should be simplified as much as possible, consisting of a set of standard objects that are connected to each other in a standardized manner to a fixed foundation.

It is important to note that a specific structure does not always correspond to a precise and exact schematic representation. Uncertainties can arise when preparing the calculation scheme, for example, due to the complexity of the structural scheme, there may not be sufficient information about the compatibility of certain joints, and the characteristics of how the interaction forces transfer between the parts of the structure can also lead to uncertainties [2].

Therefore, some analysts use what is referred to as the "principle of uncertainty in a single calculation scheme." According to this principle, multiple calculation schemes are considered to obtain the values of stresses at different cross-sections, aiming to get values that are close to the possible maximum in the given calculation scheme for all real load conditions [3]. With this approach, the reliability check is performed based on the analysis of the results obtained from several (usually two or three) calculation schemes.

If the calculation is performed using the finite element method, then preparing the calculation scheme involves collaboratively constructing a finite element model of the system being analyzed. This means that suitable elements are selected for all characteristic parts of the calculation scheme (from the standard set available in the software package), and the number of elements as well as their arrangement in the considered area is determined [4].

For all elements, it is necessary to calculate the required geometric properties and specify the material properties (such as elastic modulus, Poisson's ratio, and density).

The actual computations on the computer should only begin after compiling and verifying the complete lists of elements, actual constants, and material properties [5].

Plates are a very widely used object in construction and technology. Generally, these consist of flat bodies whose thickness is significantly smaller than their other dimensions. Therefore, Kirchhoff-Love's kinematic hypotheses can be utilized, allowing us to consider the stress state as planar (or, more precisely, generalized planar). Here, we focus on objects with constant thickness, although similar methods can also be applied to thick plates and plates with variable thickness, albeit with some difficulties.

3 RESEARCH RESULTS

The article analyzes the stress-strain state (SSS) of a parallelepiped based on the variation of the length-to-thickness ratio under different constraints and surface load distributions. To determine the influence of

changing constraint conditions and the law of surface load distribution, the following problems were solved [6].

We consider the equilibrium of a rectangular parallelepiped, where its lateral surfaces are fixed, and a uniformly distributed load $q_0 = -0.1$ MPa acts on its upper surface, while the bottom surface is free of loads.

$$\begin{cases} u_1 = 0, u_2 = 0, u_3 = 0 & \text{if } x_1 = 0, a \\ u_1 = 0, u_2 = 0, u_3 = 0 & \text{if } x_2 = 0, b \\ \sigma_{13} = 0, \sigma_{23} = 0, \sigma_{33} = q_0 & \text{if } x_3 = c \\ \sigma_{13} = 0, \sigma_{23} = 0, \sigma_{33} = 0 & \text{if } x_3 = 0 \end{cases} \quad (1)$$

We will consider the equilibrium of a rectangular parallelepiped, with the following parameters:

- $a=0.2$ m (length);
- $b=0.2$ m (width);
- $c=0.01$ m, 0.02 m, 0.04 m, 0.08 m (height);
- $E=2 \times 10^5$ MPa (elastic modulus);
- $\mu=0.3$ (Poisson's ratio);
- $\delta=20, 10, 5, 2.5$ (where $\delta=a/c$).

Due to the symmetry of the problem, we will analyze one-quarter of the parallelepiped. The problem will be solved using the finite element method, dividing the area with eight-node isoparametric elements.

The discretization parameters and the characteristics of the system of linear algebraic equations are defined with the following values:

- Number of finite elements: 2000.
- Number of nodes: 2541.
- System order: 7623.
- Half-width of the band: 402.
- Number of divisions along the Ox , Oy , Oz axes: 11, 11, 21.

In the case of a rectangular parallelepiped, the values of u_1 correspond to the values of u_2 if they are exchanged respectively in the expressions x_1 and x_2 as $a \Rightarrow b$ and $x_2 \Rightarrow x_1$. When $\gamma=1$ (where $\gamma=b/a$), the values of u_1 reach a maximum at the line $x_2=b/2$, and the values of u_2 at $x_1=a/2$. Furthermore, they are antisymmetric with respect to the main diameters, with u_1 and u_2 being positive for $x_1 < 0.5a$ and $x_2 < 0.5b$, and negative for $x_1 > 0.5a$ and $x_2 > 0.5b$, respectively. The transition u_3 is asymmetric with respect to both main diameters. Therefore, we will limit our study to the stress and deformation fields for the first quarter of the parallelepiped [7].

In the diagrams, for $x_2=0.5b$, the five values of the u_1 displacement diagrams correspond to the coordinates $x_1=0, 2, 4, 6, 8, 10$ cm, and the reference width thickness is indicated as $\delta=20; 2.5$ in two ratios.

In Figure 1, we can see that the Kirchhoff-Love hypothesis is valid for $\delta=20$, but it is relatively not satisfied for $\delta=2.5$. This indicates that the body is in a three-dimensional state [8].

From Figure 1, it follows that for $\delta=20$, the displacements u_1 and u_2 change with height according to a linear law, which demonstrates the validity of the Kirchhoff-Love hypothesis [9]. The calculation

results indicate that for $\delta=8$, the movement of u_1 is described very accurately by a linear function of height only in the segment $0.1a \leq x_1 \leq 0.9a$.

As the thickness δ decreases, the region of linear variation narrows, and the displacements at height become more concentrated; for example, for $\delta=4$, this region is located in the interval $[0.15a, 0.85a]$.

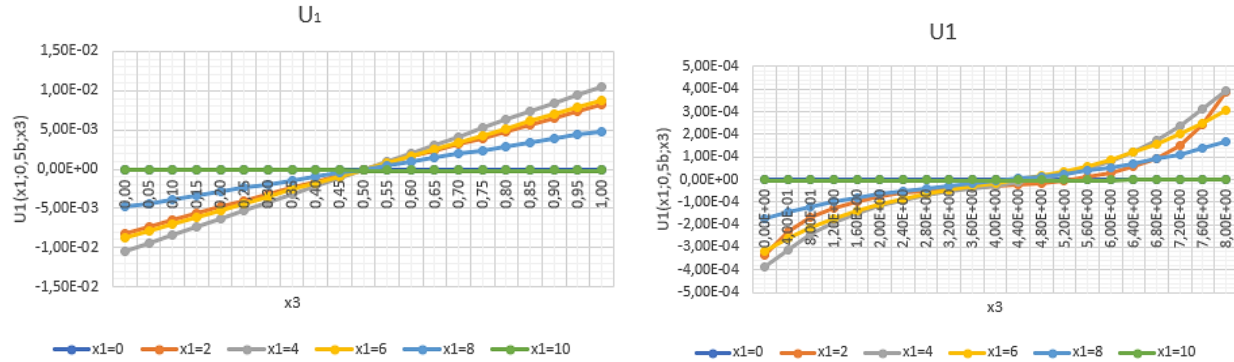


Figure 1: Change in u_1 displacement with respect to thickness.

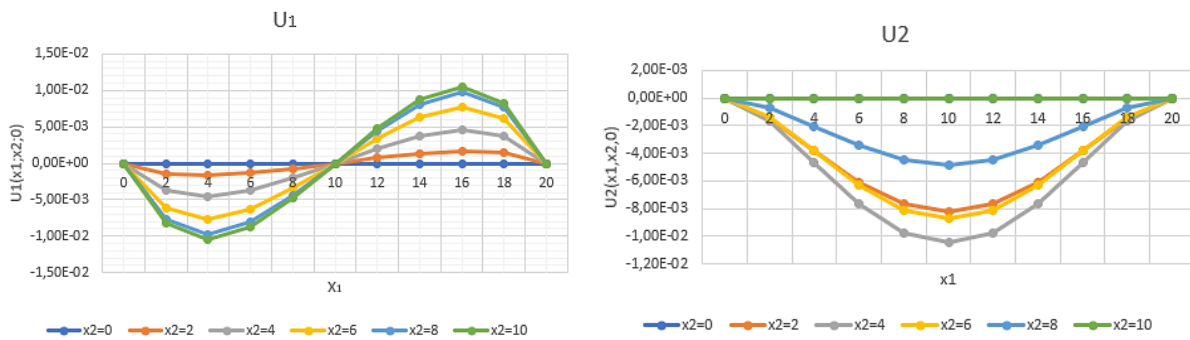


Figure 2: Variation of the values of u_1 and u_2 displacements under the influence of external force on the surface $x_3=c$.

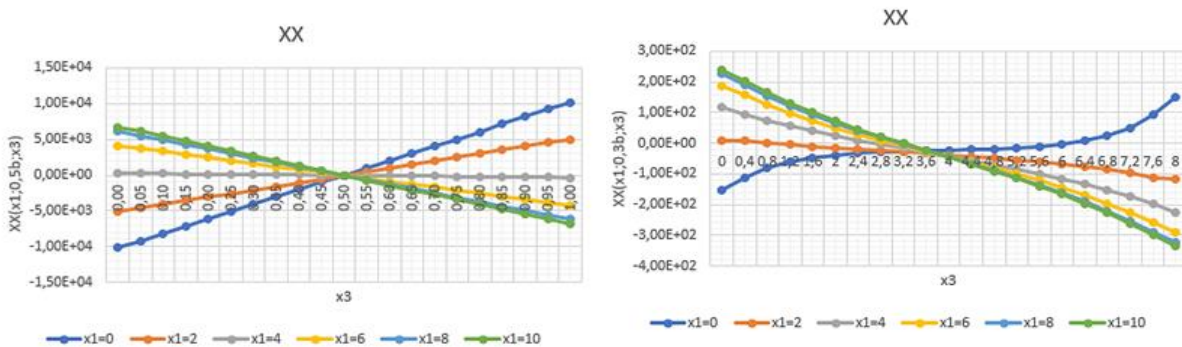


Figure 3: For the plane $x_2=0.5b$, the five values of the stress σ_{11} coordinate diagrams are given at $x_1=0, 2, 4, 6, 8, 10$ cm, and the thickness of the reference width is $\delta=20; 2.5$ for two ratios.

Table 1: Values of the displacement $U_3(x_1, 0.5b, x_3)$ with respect to the height variable x_3 and the variable $x_1 = 0, 2, 4, 6, 8, 10$ cm at $c=1$ cm.

$U_3(x_1, 0.5b, x_3)$						
X_3	$X_1=0$	$X_1=2$	$X_1=4$	$X_1=6$	$X_1=8$	$X_1=10$
0,00	0,00E+00	-2,12E-02	-6,14E-02	-1,02E-01	-1,30E-01	-1,40E-01
0,05	0,00E+00	-2,12E-02	-6,15E-02	-1,02E-01	-1,30E-01	-1,40E-01
0,10	0,00E+00	-2,11E-02	-6,15E-02	-1,02E-01	-1,30E-01	-1,40E-01
0,15	0,00E+00	-2,10E-02	-6,15E-02	-1,02E-01	-1,30E-01	-1,40E-01
0,20	0,00E+00	-2,10E-02	-6,15E-02	-1,02E-01	-1,30E-01	-1,40E-01
0,25	0,00E+00	-2,10E-02	-6,16E-02	-1,02E-01	-1,30E-01	-1,40E-01
0,30	0,00E+00	-2,09E-02	-6,16E-02	-1,02E-01	-1,30E-01	-1,40E-01
0,35	0,00E+00	-2,09E-02	-6,16E-02	-1,02E-01	-1,30E-01	-1,40E-01
0,40	0,00E+00	-2,09E-02	-6,16E-02	-1,02E-01	-1,30E-01	-1,40E-01
0,45	0,00E+00	-2,09E-02	-6,16E-02	-1,02E-01	-1,30E-01	-1,40E-01
0,50	0,00E+00	-2,09E-02	-6,16E-02	-1,02E-01	-1,30E-01	-1,40E-01
0,55	0,00E+00	-2,09E-02	-6,16E-02	-1,02E-01	-1,30E-01	-1,40E-01
0,60	0,00E+00	-2,09E-02	-6,16E-02	-1,02E-01	-1,30E-01	-1,40E-01
0,65	0,00E+00	-2,09E-02	-6,16E-02	-1,02E-01	-1,30E-01	-1,40E-01
0,70	0,00E+00	-2,09E-02	-6,16E-02	-1,02E-01	-1,30E-01	-1,40E-01
0,75	0,00E+00	-2,10E-02	-6,16E-02	-1,02E-01	-1,30E-01	-1,40E-01
0,80	0,00E+00	-2,10E-02	-6,16E-02	-1,02E-01	-1,30E-01	-1,40E-01
0,85	0,00E+00	-2,11E-02	-6,15E-02	-1,02E-01	-1,30E-01	-1,40E-01
0,90	0,00E+00	-2,11E-02	-6,15E-02	-1,02E-01	-1,30E-01	-1,40E-01
0,95	0,00E+00	-2,12E-02	-6,15E-02	-1,02E-01	-1,30E-01	-1,40E-01
1,00	0,00E+00	-2,13E-02	-6,15E-02	-1,02E-01	-1,30E-01	-1,40E-01

Table 2: Values of the displacement $U_3(x_1, 0.5b, x_3)$ with respect to the height variable X_3 and the variable $x_1 = 0, 2, 4, 6, 8, 10$ cm at $c=8$ cm.

$U_3(x_1, 0.5b, x_3)$						
X_3	$X_1=0$	$X_1=2$	$X_1=4$	$X_1=6$	$X_1=8$	$X_1=10$
0	0,00E+00	-5,30E-04	-5,30E-04	-9,96E-04	-1,36E-03	-1,59E-03
0,4	0,00E+00	-5,14E-04	-5,14E-04	-1,01E-03	-1,38E-03	-1,62E-03
0,8	0,00E+00	-5,07E-04	-5,07E-04	-1,02E-03	-1,40E-03	-1,64E-03
1,2	0,00E+00	-5,05E-04	-5,05E-04	-1,02E-03	-1,42E-03	-1,66E-03
1,6	0,00E+00	-5,07E-04	-5,07E-04	-1,03E-03	-1,43E-03	-1,68E-03
2	0,00E+00	-5,13E-04	-5,13E-04	-1,04E-03	-1,44E-03	-1,70E-03
2,4	0,00E+00	-5,20E-04	-5,20E-04	-1,04E-03	-1,46E-03	-1,71E-03
2,8	0,00E+00	-5,29E-04	-5,29E-04	-1,06E-03	-1,47E-03	-1,73E-03
3,2	0,00E+00	-5,39E-04	-5,39E-04	-1,07E-03	-1,49E-03	-1,75E-03
3,6	0,00E+00	-5,50E-04	-5,50E-04	-1,09E-03	-1,51E-03	-1,77E-03
4	0,00E+00	-5,62E-04	-5,62E-04	-1,10E-03	-1,53E-03	-1,79E-03
4,4	0,00E+00	-5,76E-04	-5,76E-04	-1,12E-03	-1,55E-03	-1,81E-03
4,8	0,00E+00	-5,90E-04	-5,90E-04	-1,15E-03	-1,57E-03	-1,83E-03
5,2	0,00E+00	-6,07E-04	-6,07E-04	-1,17E-03	-1,60E-03	-1,85E-03
5,6	0,00E+00	-6,25E-04	-6,25E-04	-1,20E-03	-1,62E-03	-1,88E-03
6	0,00E+00	-6,47E-04	-6,47E-04	-1,23E-03	-1,65E-03	-1,90E-03
6,4	0,00E+00	-6,72E-04	-6,72E-04	-1,26E-03	-1,67E-03	-1,92E-03
6,8	0,00E+00	-7,03E-04	-7,03E-04	-1,30E-03	-1,70E-03	-1,94E-03
7,2	0,00E+00	-7,41E-04	-7,41E-04	-1,33E-03	-1,72E-03	-1,96E-03
7,6	0,00E+00	-7,90E-04	-7,90E-04	-1,36E-03	-1,74E-03	-1,98E-03
8	0,00E+00	-8,52E-04	-8,52E-04	-1,38E-03	-1,76E-03	-1,99E-03

Table 3: Comparison of the values of displacement U_3 according to two theories.

δ	20	10	8	6	4	2
According to three-dimensional theory.	11.127	1.584	0.878	0.431	0.180	0.066
According to two-dimensional theory.	11.059	1.382	0.707	0.297	0.084	0.011

 Table 4: Comparison of the values of stress σ_{11} according to two theories.

$\sigma_{11}(0, 0.5b, x_3)$				
δ	According to three-dimensional theory		According to two-dimensional theory	
	$X_3=c$	$X_3=0$	$X_3=c$	$X_3=0$
20	-107.36	107.50	-123.20	123.20
10	-31.00	30.97	-30.80	30.80
8	-20.88	20.77	-19.71	19.71
6	-12.76	12.50	-11.09	11.09
4	-6.77	6.25	4.93	4.93
2	-3.13	1.97	-1.23	1.23

In Figure 2, the variation of $u_1(x_1, 0.5b, x_3)$ displacement at a height of $\delta=2.5$ is shown, along with the five values of x_1 (where $x_1=0, 2, 4, 6, 8, 10$ cm corresponding to curves 1-6). From this figure, it can be concluded that at $\delta=2.5$, the distribution character of stress and displacement fields is primarily three-dimensional.

If we look at Table 1, it presents the variation of $U_3(x_1, 0.5b, x_3)$ displacement with respect to height. According to the Kirchhoff-Love hypothesis, the value of U_3 should remain constant. Comparing the values in the table, it is evident that this hypothesis is valid, as three of the values match, with a difference equal to 0.001.

A detailed analysis of the results shows that U_3 tends to vary significantly between any plane at $x_3=\text{const}$ and at the heights along the line $(0.5a, 0.5b, z=c)$, where $0.5 \leq z \leq 1$ and z rapidly approaches as the value of δ decreases.

If we pay attention to Table 2, it presents the variation of $U_3(x_1, 0.5b, x_3)$ displacement with respect to height. According to the Kirchhoff-Love hypothesis, the value of U_3 should remain constant; however, comparing the values in the table indicates that this hypothesis is not valid. In this case, the body is changing according to a three-dimensional law [5].

In the figures, for the plane $x_2=0.5b$, the stress diagrams σ_{11} show five values of $x_1=0, 2, 4, 6, 8, 10$ cm, with two thickness ratios given at $\delta=20$ and $\delta=2.5$. In Figure 3, we can see that the Kirchhoff-Love hypothesis holds at $\delta=20$, but it is not satisfied at $\delta=2.5$, indicating that the body is in a three-dimensional state.

Table 3 shows the values of U_3 obtained from the three-dimensional and two-dimensional theories for the bending of a square plate (compressed along the

contour) with the same data [6]. It is clear from Table 3 that there is good agreement between the two theories at large values of δ . Table 4 shows the values of σ_{11} obtained from the three-dimensional and two-dimensional theories for the bending of a square plate (compressed along the contour) with the same data [6]. It is clear from Table 4 that there is good agreement between the two theories at large values of δ .

4 CONCLUSIONS

This paper proposes a comprehensive analysis of the elastic stress-strain performance of complex-shaped three-dimensional bodies, with particular focus on parallelepipeds subjected to varying thickness-to-length ratios (δ). The results demonstrate that for bodies with δ greater than 8, the Kirchhoff-Love hypothesis remains valid across most regions except near the edges and concentrated loading zones, with displacement components u_1 and u_2 , and stresses σ_{11} , σ_{12} and σ_{22} exhibiting planar behavior. However, as δ decreases to values less than or equal to 4, significant three-dimensional effects arise, particularly in components such as u_3 , σ_{13} , σ_{23} , and σ_{33} , which follow parabolic distributions through the thickness and peak at mid-plane sections, necessitating full 3D modeling. The use of the finite element method with eight-node isoperimetric elements proved effective in capturing these behaviors, and the simulation results aligned well with theoretical expectations, validating both the numerical formulation and mesh discretization. Furthermore, comparative data between two-dimensional and three-dimensional models confirmed the reliability of the former only at high δ

values, highlighting the limitations of classical plate theory for thicker or complex geometries. The influence of boundary conditions and load distribution was also found to be critical in defining the deformation patterns, underscoring the need for precise model setup in structural simulations. Finally, this work reinforces the importance of advanced numerical methods in accurately assessing the mechanical performance of engineering structures and provides a foundation for future studies involving elastoplastic behavior, heterogeneous materials, and geometrically intricate domains.

REFERENCES

- [1] A. A. Samarskiy, *Introduction to Numerical Methods*, 2nd ed., Moscow: Lan', 2009.
- [2] H. Alkattan, M. Abotaleb, A. A. Subhi, O. A. Adelaja, A. Kadi, and H. K. Ibrahim Al-Mahdawi, "The prediction of students' academic performances with a classification model built using data mining techniques," in *IET Conference Proceedings CP824*, vol. 2022, no. 26, pp. 353-356, Stevenage, UK: The Institution of Engineering and Technology, 2022.
- [3] A. N. Fedorenko, B. N. Fedulov, and E. V. Lomakin, "Problem of loss of stability of thin-walled structures made of composite materials, the properties of which depend on the type of loading," *PNRPU Mechanics Bulletin*, vol. 3, no. 12, pp. 104-111, 2019.
- [4] E. M. Morozov and G. P. Nikishkov, *Finite Element Method in Fracture Mechanics*, Moscow: Nauka, 1980.
- [5] S. Cheremnykh, "Experimental study of elastic-plastic deformation of a cylindrical shell made of 45 steel," *Structural Mechanics of Engineering Constructions and Buildings*, vol. 5, no. 17, pp. 519-527, 2021.
- [6] F. C. Onyeka and B. O. Mama, "Analytical study of bending characteristics of an elastic rectangular plate using direct variational energy approach with trigonometric function," *Emerging Science Journal*, vol. 5, no. 6, pp. 916-930, Dec. 2021, ISSN: 2610-9182.
- [7] V. Vlasov, *Selected Works*, Moscow: Nauka, 1964.
- [8] G. Kirchhoff, *On the Equilibrium and Motion of an Elastic Disk*, Berlin: De Gruyter, 1850.
- [9] M. Rasilmukhamedov, A. Boltaev, and A. Tukhtakhodjaev, "Modeling of the electronic document circulation and record keeping system in the processes of cargo transportation in railway transport," in *E3S Web of Conferences*, Voronezh, 2023.
- [10] A. Abdulkarem and A. Krivtsun, "An analysis of automated essay scoring frameworks," *IJApSc*, vol. 1, no. 3, pp. 71-81, Dec. 2024, doi: 10.69923/av1gt264.